Protein Cell 2013, 4(4): 286–298
DOI 10.1007/s13238-013-2116-z

Protein & Cell

RESEARCH ARTICLE

Plasma membrane calcium ATPase 4b inhibits nitric oxide generation through calcium-induced dynamic interaction with neuronal nitric oxide synthase

Wenjuan Duan[1*], Juefei Zhou[1,2*], Wei Li [3*], Teng Zhou[1,4], Qianqian Chen[1,4], Fuyu Yang[1✉], Taotao Wei[1✉]

[1] National Laboratory of Biomacromolecules, Institute of Biophysics, Chinese Academy of Sciences, Beijing 100101, China
[2] Research Department of Bacterial Vaccine, Chengdu Institute of Biological Products Co. Ltd, Chengdu 610023, China
[3] State Key Laboratory of Virology, Wuhan Institute of Virology, Chinese Academy of Sciences, Wuhan 430071, China
[4] University of Chinese Academy of Sciences, Beijing 100049, China
✉ Corresponding authors: yangfy@sun5.ibp.ac.cn (F. Yang), weitt@moon.ibp.ac.cn (T. Wei)
Received November 12, 2013 Accepted February 15, 2013

ABSTRACT

The activation and deactivation of Ca^{2+}- and calmodulin-dependent neuronal nitric oxide synthase (nNOS) in the central nervous system must be tightly controlled to prevent excessive nitric oxide (NO) generation. Considering plasma membrane calcium ATPase (PMCA) is a key deactivator of nNOS, the present investigation aims to determine the key events involved in nNOS deactivation of by PMCA in living cells to maintain its cellular context. Using time-resolved Förster resonance energy transfer (FRET), we determined the occurrence of Ca^{2+}-induced protein–protein interactions between plasma membrane calcium ATPase 4b (PMCA4b) and nNOS in living cells. PMCA activation significantly decreased the intracellular Ca^{2+} concentrations ($[Ca^{2+}]_i$), which deactivates nNOS and slowdowns NO synthesis. Under the basal $[Ca^{2+}]_i$ caused by PMCA activation, no protein-protein interactions were observed between PMCA4b and nNOS. Furthermore, both the PDZ domain of nNOS and the PDZ-binding motif of PMCA4b were essential for the protein-protein interaction. The involvement of lipid raft microdomains on the activity of PMCA4b and nNOS was also investigated. Unlike other PMCA isoforms, PMCA4 was relatively more concentrated in the raft fractions. Disruption of lipid rafts altered the intracellular localization of PMCA4b and affected the interaction between PMCA4b and nNOS, which suggest that the unique lipid raft distribution of PMCA4 may be responsible for its regulation of nNOS activity. In summary, lipid rafts may act as platforms for the PMCA4b regulation of nNOS activity and the transient tethering of nNOS to PMCA4b is responsible for rapid nNOS deactivation.

KEYWORDS plasma membrane calcium ATPase, neuronal nitric oxide synthase, calcium, nitric oxide, lipid raft, Förster resonance energy transfer

INTRODUCTION

Nitric oxide (NO) is synthesized from oxygen and l-arginine by nitric oxide synthase (NOS) and has essential roles in vascular tone modulation, neurotransmission, and immune defense (Moncada and Bolanos, 2006). Three genetically different isoforms of NOS account for NO production, namely, the two constitutive forms endothelial nitric oxide synthase (eNOS) and neuronal nitric oxide synthase (nNOS) and the inducible form inducible nitric oxide synthase (iNOS). Among these isoforms, nNOS (also known as NOS-I) is the isoform predominantly found in neuronal tissue (Alderton et al., 2001). NO production by activated nNOS in the central nervous system is triggered by elevated intracellular Ca^{2+} concentrations ($[Ca^{2+}]_i$) and it has been associated with the induction and maintenance of synaptic plasticity. NO may also regulate neurosecretory control (Calabrese et al., 2007). However, aside from the physiologic functions mentioned above, NO becomes noxious when produced in excess (Pacher et al., 2007). Superfluous NO has

*These authors contributed equally to the work.

© Higher Education Press and Springer-Verlag Berlin Heidelberg 2013

been closely associated with the risk of the developing brain ischemia damage, Parkinson's disease, Alzheimer's disease, and other nervous system diseases (Torreilles et al., 1999; Tran et al., 2003; Moro et al., 2004; Guix et al., 2005). Based on the physiologic and pathologic role of NO, the generation, release, diffusion, and deactivation of NO should be precisely regulated in the central nervous system, which is accomplished mainly through nNOS activation and deactivation.

The NO synthesis catalyzed by nNOS is Ca^{2+}-dependent and the regulation of nNOS activity is closely related to the structure of nNOS. The nNOS monomer (inactive form) has a bidomain structure, wherein an oxygenase domain (N-terminus) that contains binding sites for heme, BH_4, and l-arginine is linked by a calmodulin-binding motif to a reductase domain (C-terminus) that contains binding sites for FAD, FMN, and NADPH (Alderton et al., 2001; Sagami et al., 2001; Zhou and Zhu, 2009). In addition, the N-terminus of nNOS contains a PDZ domain that participates in the formation of active dimers and interacts with other proteins in the specific regions of the cell (Zhou and Zhu, 2009). nNOS is anchored to the second PDZ domain of PSD-95 through the interaction between the PDZ domains, while PSD-95 is bound to NMDA receptors (NMDA-R) through the PDZ domain. This indirect anchoring positions nNOS and NMDA-R close to each other, thereby greatly increasing the efficiency of the conversion from excitatory amino acids signals to NO signals (Brenman et al., 1996). Meanwhile, excess NO leads to the nitrosylation of the Cys^{744} and Cys^{798} of the NMDA-R, which deactivates NMDA-R and decreases Ca^{2+} influx (Kim et al., 1999). Therefore, the contiguity of nNOS and NMDA-R increases the sensitivity and speed of negative feedback regulation.

Compared with nNOS activation, less is known about the key events during nNOS deactivation. Using biochemical approaches, Schuh et al. found that the PDZ binding motif at the C-terminus of plasma membrane calcium ATPase 4b (PMCA4b) interacts with the PDZ domain of nNOS. Based on these findings, Schuh suggested that PMCA is a major factor that downregulates nNOS activity (Schuh et al., 2001).

In the present investigation, we used time-resolved Förster resonance energy transfer (FRET) to monitor the transient protein-protein interactions between PMCA and nNOS in living cells and simultaneously monitored the changes in intracellular Ca^{2+} concentrations ($[Ca^{2+}]_i$) and NO concentrations ($[NO]_i$). We found that the increase in $[Ca^{2+}]_i$-induced protein-protein interaction between PMCA4b and nNOS contributes to nNOS deactivation. We also found that the interaction between PMCA4b and nNOS depends on the PDZ domain and the integrity of the lipid rafts. These events may play an important role in controlling NO production in the central nervous system.

RESULTS

Expression and partitioning profiles of PMCA isoforms in rat brains

We first analyzed the expression profiles of the four PMCA isoforms (PMCA1, PMCA2, PMCA3, and PMCA4) in adult rat brains at both the mRNA level and the protein level. The four PMCA isoforms were expressed in the four functional regions of the brain we tested, namely, the cerebral cortex, cerebellar cortex, hippocampus, and corpus striatum, as shown in Fig. 1A and 1B. Then, we investigated the partitioning of these PMCA isoforms in the brain plasma membrane microdomains. We fractionated the brain plasma membrane using the methods described by Sepúlveda et al. (2006), and found that all four PMCA isoforms are associated with the low density fractions (lipid raft microdomains); however, PMCA4 was relatively enriched in the lipid rafts compared with the other isoforms (Fig. 1C).

Impairment of lipid rafts affected the localization of PMCA4 and nNOS

nNOS expression was relatively higher in the cerebellum (Fig. 2A); thus, we used primary cerebellar granule cells, a relatively homogenous and well-characterized culture system of cerebellar neurons (Dudek et al., 1997), to investigate the subcellular localization of endogenous PMCA4 and nNOS in neuronal cells. We also observed the subcellular localization of nNOS in HEK-293 cells transfected with pcDNA3.1-nNOS vector. The immunofluorescence images clearly indicate that PMCA4 has typical membrane protein distribution, whereas the endogenous and exogenous nNOS have cytoplasmic distributions (Fig. 2B).

The intracellular localization of PMCA and nNOS was further investigated in living cells that expressed fused proteins. The HEK-293 cells transfected with pEGFP-hPMCA4b and pRFP-nNOS were used to observe the localization of PMCA4 and nNOS. The intracellular distribution patterns of PMCA4b-EGFP and nNOS-RFP were similar to the immunocytochemistry results, as shown in Fig. 2C. The merged image indicated the partial colocalization of PMCA4b-EGFP and nNOS-RFP at the plasma membrane.

The cell fractionation results indicate that PMCA4 is relatively enriched in lipid rafts; hence, we investigated the influence of lipid rafts on the intracellular localization of PMCA4 and nNOS. After treatment with MβCD, the lipid raft microdomains of the plasma membrane were disrupted and the membrane lipids were remodeled. Consequently, PMCA4b was redistributed in the plasma membrane, forming a relatively homogenous pattern, whereas nNOS was dispersed in the cytoplasm, which caused the disappearance of the partial colocalization of PMCA4b-EGFP and nNOS-RFP.

Increase in $[Ca^{2+}]_i$ activated PMCA and nNOS in living cells

We measured the activity of PMCA and nNOS in living cells using Ca^{2+}-specific Fura-2-AM and NO-specific DAF-2-DA fluorescence probes, respectively. Isosmotic buffer containing *N*-methyl-d-glucamine was used to block the Ca^{2+} transport mediated by the Na^+-Ca^{2+} exchanger (NCX), whereas thapsigargin was added to inhibit the activity of the endoplasmic re-

© Higher Education Press and Springer-Verlag Berlin Heidelberg 2013

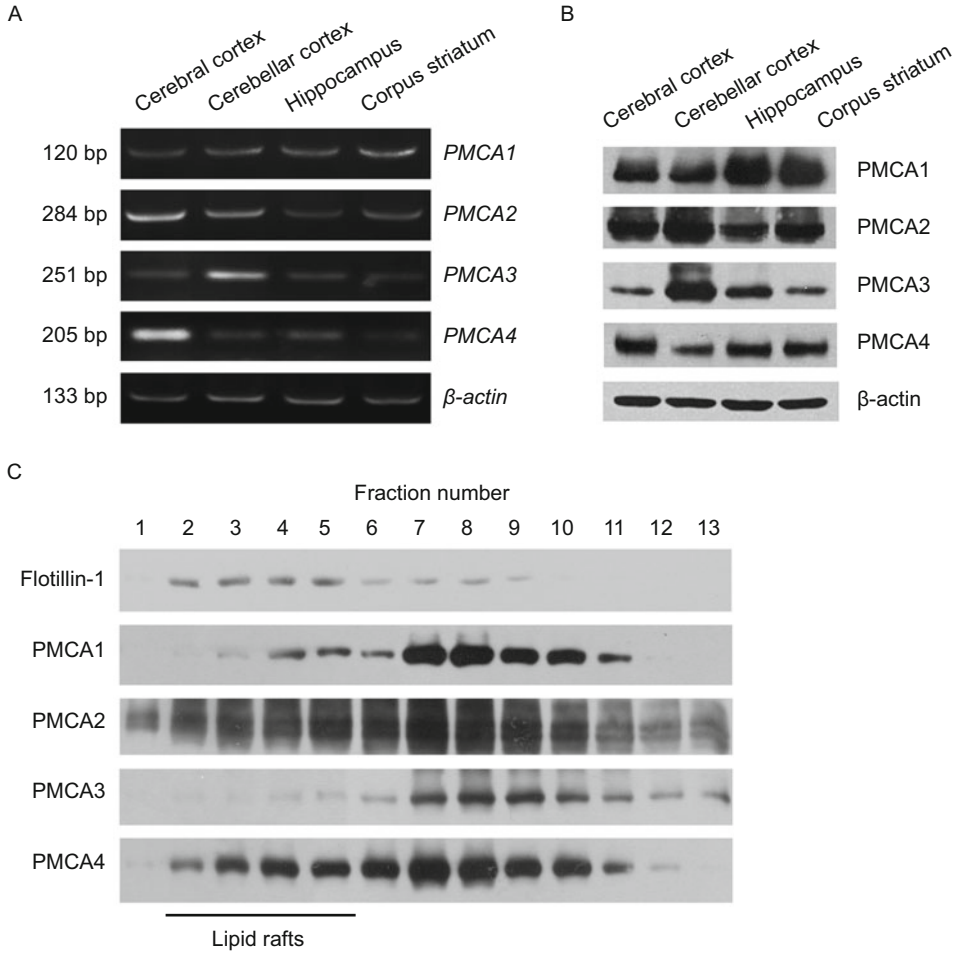

Figure 1. Expression and partitioning profiles of four PMCA isoforms in adult rat brains. (A) mRNA expression profiles of four PMCA isoforms. RNA was isolated from the cerebral cortex, cerebellar cortex, hippocampus, and corpus striatum and subjected to RT-PCR to analyze the expression of PMCA1, PMCA2, PMCA3, and PMCA4. β-Actin was used as the internal standard. (B) Protein expression profiles of the four PMCA isoforms. Proteins were extracted from the cerebral cortex, cerebellar cortex, hippocampus, and corpus striatum, and 20 μg of each sample was subjected to SDS-PAGE and immunoblotted with antibodies against PMCA1, PMCA2, PMCA3, and PMCA4. β-Actin was used as the internal standard. (C) Partitioning of the four PMCA isoforms in the microdomains of the plasma membrane of neuronal cells. The plasma membrane was fractionized into lipid rafts or non-raft fractions using a Nycodenz density gradient. Approximately, 11 μL of the 13 fractions was subjected to 7.5% SDS-PAGE and immunoblotted with antibodies against the PMCA isoforms. Flotillin-1 was used as the marker for lipid raft fractions.

ticulum Ca^{2+}-ATPase. In the presence of *N*-methyl-d-glucamine and thapsigargin, the decrease in $[Ca^{2+}]_i$ solely depends on PMCA activation.

We first measured the activity of endogenous PMCA and nNOS in cerebellar granule cells by monitoring the changes in $[Ca^{2+}]_i$ and $[NO]_i$. After the addition of glutamate, the glutamate receptor on the plasma membrane was activated and the receptor-coupled Ca^{2+} channel was opened, causing a rapid influx of Ca^{2+} into the cells. The drastic increase in $[Ca^{2+}]_i$ rapidly activated the PMCA, which transports Ca^{2+} out of the cells. The PMCA activation gradually returns $[Ca^{2+}]_i$ to the quiescent levels (Fig. 3A). High $[Ca^{2+}]_i$ levels also activate nNOS, triggers NO generation (Fig. 3C). The MβCD treatment markedly slowed down the decrease in $[Ca^{2+}]_i$ (Fig. 3B), and the glutamate-treated cerebellar granule cells were unable to generate NO (Fig. 3D), which suggests that the integrity of lipid rafts also has an important role in the activation of PMCA and nNOS.

Subsequently, we measured the changes in $[Ca^{2+}]_i$ and $[NO]_i$ in HEK-293 cells. Exposure of HEK-293 cells to thapsigargin and ionomycin triggered the release of Ca^{2+} from the endoplasmic reticulum and significantly increased the $[Ca^{2+}]_i$, which rapidly activated PMCA. Activated PMCA gradually decreased the $[Ca^{2+}]_i$ to basal levels (Fig. 4A). High $[Ca^{2+}]_i$ levels also activated nNOS in the HEK-293 cells transfected with pcDNA3.1-nNOS, which triggered the generation of NO (Fig. 4C). Treatment with MβCD also limited the elimination of Ca^{2+} (Fig. 4B)

© Higher Education Press and Springer-Verlag Berlin Heidelberg 2013

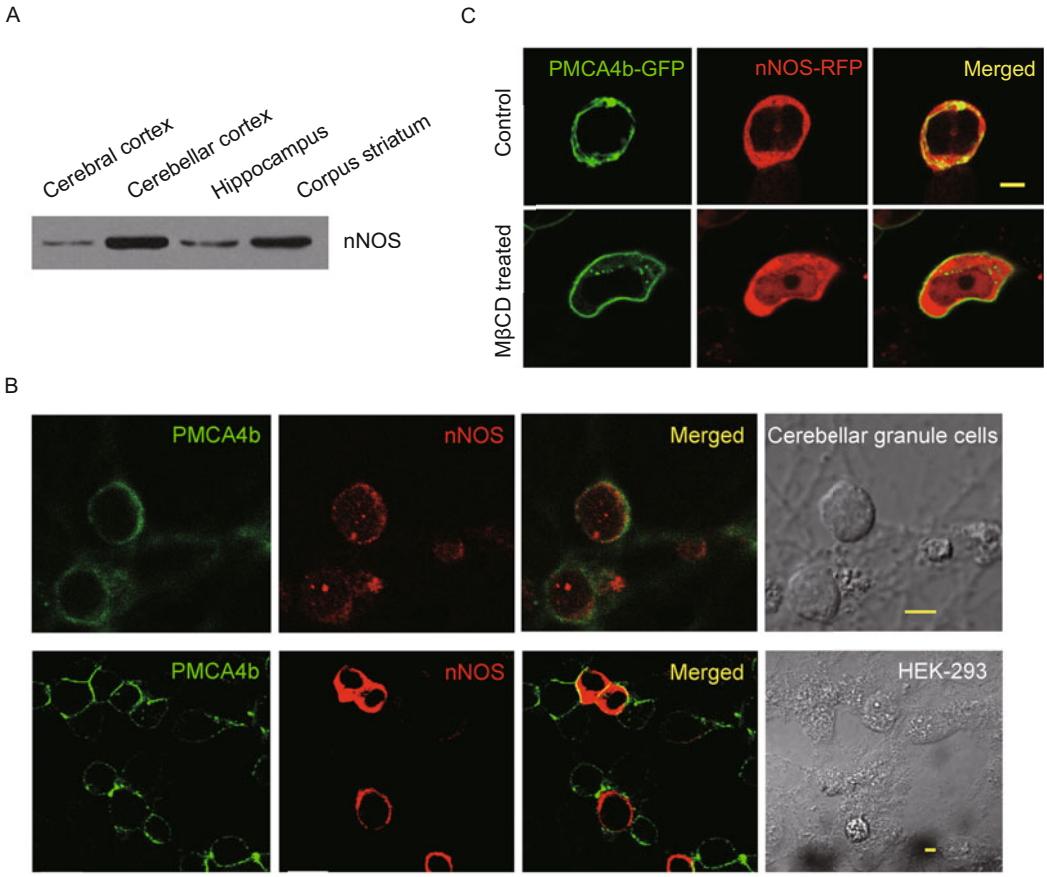

Figure 2. Intracellular localization of PMCA4b and nNOS in cerebellar granule cells and HEK-293 cells. (A) Protein expression profiles of nNOS. Proteins were extracted from the cerebral cortex, cerebellar cortex, hippocampus, and corpus striatum. Then, 20 μg of each sample was subjected to SDS-PAGE and then immunoblotted with antibodies against nNOS. (B) Immunofluorescence micrographs of primary cerebellar granule cells and HEK-293 cells transfected with pcDNA3.1-nNOS. Red, nNOS; green, PMCA4b. (C) Fluorescence micrographs of PMCA4b (fused with EGFP) and nNOS (fused with RFP) expression in HEK-293 cells. HEK-293 cells were cotransfected with pEGFP-hPMCA4b and pRFP-nNOS. In some experiments, the cells were pretreated with MβCD to disrupt lipid raft integrity. Bar, 5 μm.

and blocked the generation of NO (Fig. 4D).

Increased PMCA activity decreased NO generation

We cotransfected HEK-293 cells with different amounts of pcDNA3.1-myc-PMCA4b and with 1 μg of pcDNA3.1-nNOS to manipulate their PMCA activity. Exposure of cells to thapsigargin and ionomycin triggered the Ca^{2+}-dependent activation of PMCA and nNOS. Transfection with pcDNA3.1-myc-PMCA4b plasmids caused the dose-dependent expression of exogenous PMCA4b proteins, as shown in Fig. 5A. In addition, the increase in PMCA4b protein levels was correlated with the increase in PMCA activity (Fig. 5B). Transfecting more PMCA4b expression plasmids increased the Ca^{2+}-elimination speed. The total PMCA activity of HEK-293 cells transfected with 2 μg of PMCA4b plasmids was about twice that of cells transfected with empty vectors.

We also detected the nNOS-generated NO in HEK-293 cells simultaneously cotransfected with pcDNA3.1-nNOS and pcDNA3.1-myc-PMCA4b, and found that HEK-293 cells with higher PMCA4b activities generated less NO (Fig. 5C). These results suggest that PMCA4b is one of the key molecules that deactivated nNOS.

Ca^{2+}-induced transient protein-protein interaction between PMCA4b and nNOS was mediated by PDZ domain and depended on the integrity of lipid rafts

Construction of vectors and intracellular localization of fused proteins

Time-resolved FRET was used in living cells to study the protein–protein interaction between PMCA4b and nNOS under physiologic conditions. EGFP fused with PMCA4b and RFP fused with nNOS were used as donor–acceptor pairs. A series of vectors that encode the fused EGFP and PMCA4b protein or the fused RFP and nNOS protein were constructed with pEGFP-N1 vector or pDsRed/monomer C1 vector, respec-

© Higher Education Press and Springer-Verlag Berlin Heidelberg 2013

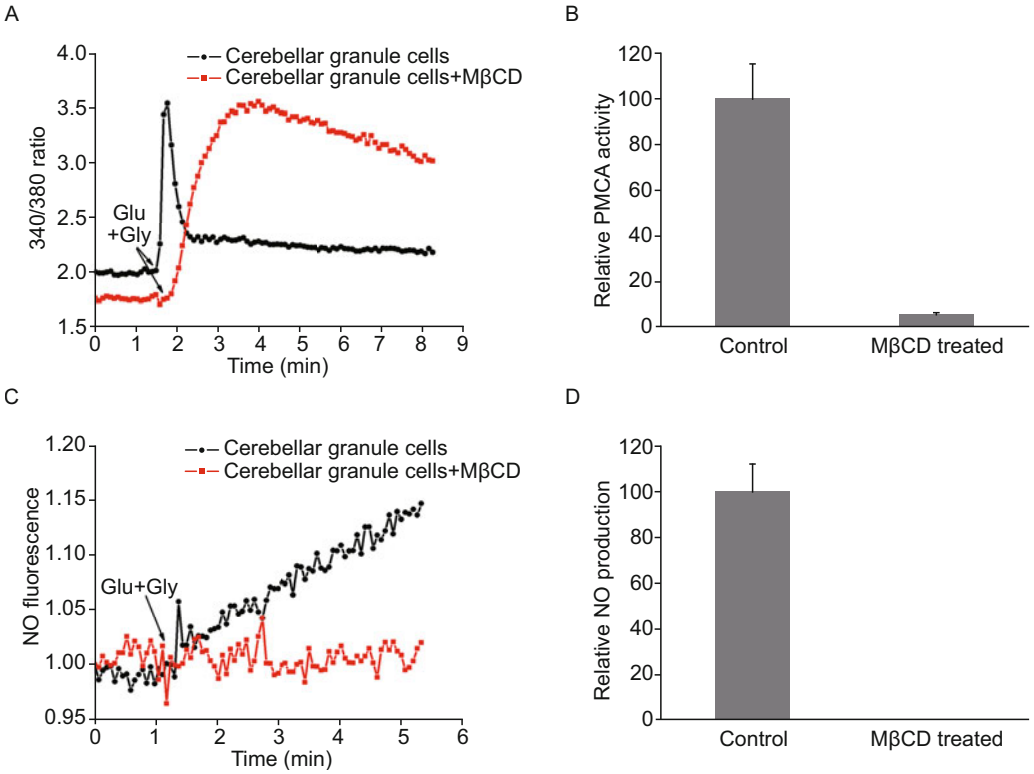

Figure 3. Changes in $[Ca^{2+}]_i$ and $[NO]_i$ in cerebellar granule cells. (A) Glutamate-induced increase in $[Ca^{2+}]_i$ in cerebellar granule cells. Primary cerebellar granule cells were loaded with a Ca^{2+}-sensitive cell-permeable Fura-2-AM probe, and then treated with glutamate and glycine. The changes in fluorescence at 340 nm/380 nm excitation and 510 nm emission wavelengths were recorded under a Nikon TE2000 fluorescence microscope. Glutamate/glycine caused a drastic increase in $[Ca^{2+}]_i$ via the activation of glutamate receptor. (B) Quantitative determination of PMCA activity. Increased $[Ca^{2+}]_i$ activates PMCA, which causes a rapid decrease in $[Ca^{2+}]_i$. The speed of Ca^{2+} efflux from cells reflects PMCA activity. Disruption of lipid rafts by MβCD causes a marked decrease in PMCA activity. (C) Glutamate-induced increase in $[NO]_i$ in cerebellar granule cells. Primary cerebellar granule cells were loaded with the NO-sensitive cell-permeable DAF-2-DA probe and then treated with glutamate and glycine. The changes in fluorescence at 490 nm excitation and 520 nm emission wavelengths were recorded under a Nikon TE2000 fluorescence microscope. (D) Quantitative determination of nNOS activity. Disruption of lipid rafts by MβCD markedly decreased nNOS activity.

tively (Fig. 6A). The pEGFP-hPMCA4b-mut vector carried an Asp^{672}→Glu mutation that reduced the ATPase activity to about 10%. The pEGFP-hPMCA4b-cap vector contained a myc/6× His tag at the C-terminus of PMCA4b, which blocks the binding to PDZ domains (Adamo et al., 1995). The pRFP-ΔnNOS vector, which encodes a fused nNOS-RFP protein with a deleted PDZ-domain, was also constructed to investigate the involvement of PDZ domain in the protein-protein interactions between PMCA4b and nNOS. The intracellular localization of fused proteins was examined under confocal microscopy. Neither the mutation of Asp^{672}→Glu nor the myc/6× His tag affected the membrane localization of PMCA (Fig. 6B).

Ca^{2+}-induced transient protein-protein interaction between PMCA4b and nNOS

We investigated the protein-protein interaction between PMCA4b and nNOS in HEK-293 cells transfected with vectors that encode the fused PMCA4b and nNOS protein. The time course of the occurrence of FRET is shown in Fig. 6C. In quiescent cells with low $[Ca^{2+}]_i$, both PMCA and nNOS were kept in inactive form and no energy transfer occurred between hPMCA4b-EGFP and nNOS-RFP. However, when the cells were treated with thapsigargin and ionomycin, the Ca^{2+} was released from intracellular calcium pools (mainly form endoplasmic reticulum) into the cytoplasm and the $[Ca^{2+}]_i$ reached high levels. Under these conditions, both PMCA4b and nNOS were activated. At 30 s after the addition of thapsigargin and ionomycin, the fluorescence intensity of PMCA4b-EGFP decreased, whereas that of nNOS-RFP increased, which suggests the occurrence of FRET between PMCA4b-EGFP and nNOS-RFP. That is, thapsigargin and ionomycin treatment initiated the increase in $[Ca^{2+}]_i$, which triggered the protein–protein interaction between PMCA4b and nNOS. Interestingly, the protein–protein interaction between PMCA4b and nNOS was highly dynamic and dependent on $[Ca^{2+}]_i$. At 160 s after the addition of thapsigargin and ionomycin, the $[Ca^{2+}]_i$ decreased

 © Higher Education Press and Springer-Verlag Berlin Heidelberg 2013

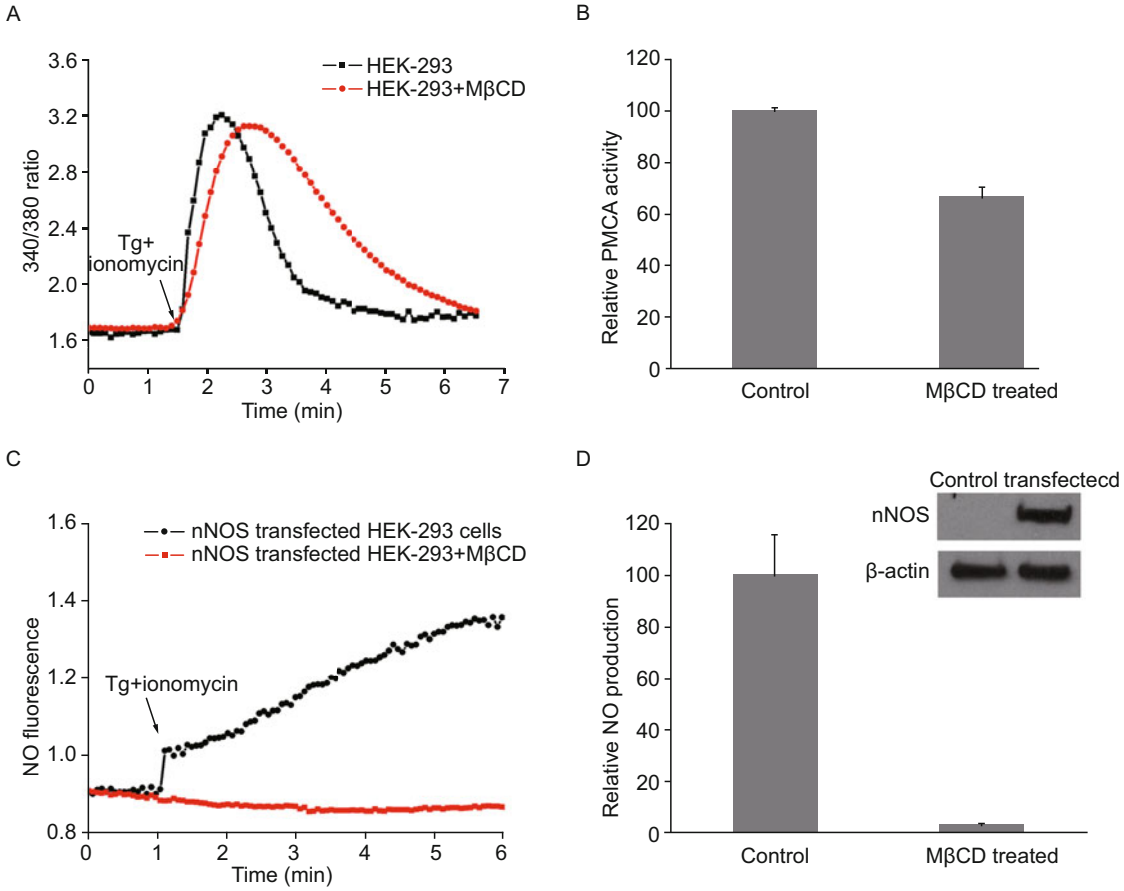

Figure 4. Changes in $[Ca^{2+}]_i$ and $[NO]_i$ in HEK-293 cells. (A) Thapsigargin and ionomycin-induced increase in $[Ca^{2+}]_i$ in HEK-293 cells. HEK-293 cells were transfected with pcDNA3.1-nNOS for 48 h, loaded with the Ca^{2+}-sensitive cell-permeable Fura-2-AM probe and then treated with thapsigargin and ionomycin. The changes in fluorescence at 340/380 nm were recorded under a Nikon TE2000 fluorescence microscope. Thapsigargin and ionomycin drastically increased the $[Ca^{2+}]_i$. (B) Quantitative determination of PMCA activity. The increased $[Ca^{2+}]_i$ activates PMCA, which rapidly decreased the $[Ca^{2+}]_i$. The speed of Ca^{2+} efflux reflects the PMCA activity. Disruption of lipid rafts by MβCD markedly decreased the PMCA activity. (C) Calcium-dependent, thapsigargin and ionomycin-induced increase in $[NO]_i$ in HEK-293 cells. HEK-293 cells transfected with pcDNA3.1-nNOS were loaded with the NO-sensitive cell-permeable DAF-2-DA probe and then treated with thapsigargin and ionomycin. The changes in fluorescence intensity from 510 nm to 540 nm were recorded under a Nikon TE2000 fluorescence microscope. (D) Quantitative determination of nNOS activity. Disruption of lipid rafts by MβCD marked decreased the nNOS activity.

to basal levels and the FRET between PMCA4b-EGFP and nNOS-RFP disappeared.

Comparison of the FRET that occurred between hPMCA4b-EGFP/nNOS-RFP and hPMCA4b-mut-GFP/nNOS-RFP revealed that the maximal nF of the HEK-293 cells transfected with pEGFP-hPMCA4b-mut (lower ATPase activity) was 54, whereas that of the HEK-293 cells transfected with pEGFP-hPMCA4b (normal ATPase activity) was 42. The difference in FRET intensity may be due to the difference in PMCA activity. The overexpression of functional hPMCA4b fused proteins enhanced PMCA activity, which increased the Ca^{2+}-elimination machinery. The rapid decline in $[Ca^{2+}]_i$ in the HEK-293 cells transfected with pEGFP-hPMCA4b significantly decreased the protein–protein interaction between PMCA4b and nNOS.

Importance of the PDZ domain and the lipid rafts in the protein-protein interaction between PMCA4b and nNOS

We further investigated the effects of the PDZ domain of nNOS and the PDZ-binding motif of PMCA4b on the protein–protein interaction between PMCA4b and nNOS. The PDZ domain of nNOS (1–299 aa) was deleted by constructing the vector pRFP-ΔnNOS. Transfection with the vector pEGFP-hPMCA4b-cap blocked the binding of the myc/6× His tag at the C-terminus of PMCA4b to the PDZ domains (Adamo et al., 1995). No apparent FRET was observed in the HEK-293 cells cotransfected with pEGFP-hPMCA4b-cap plus pRFP-nNOS, or pEGFP-hPMCA4b-mut plus pRFP-ΔnNOS, which suggests that both the C-terminus PDZ binding motif of PMCA4b and the PDZ domain of nNOS were crucial for the protein–protein

© Higher Education Press and Springer-Verlag Berlin Heidelberg 2013

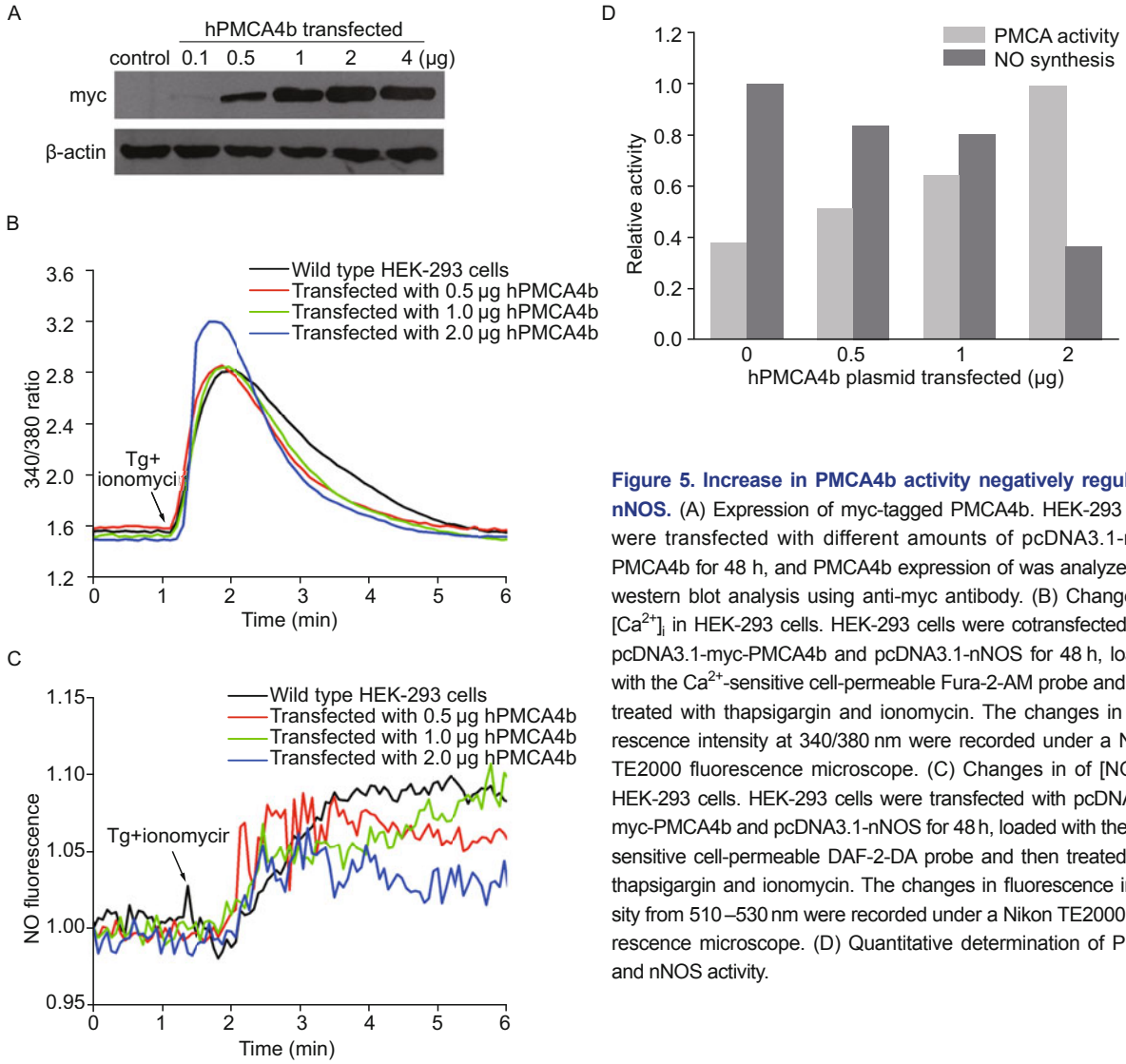

Figure 5. Increase in PMCA4b activity negatively regulates nNOS. (A) Expression of myc-tagged PMCA4b. HEK-293 cells were transfected with different amounts of pcDNA3.1-myc-PMCA4b for 48 h, and PMCA4b expression of was analyzed via western blot analysis using anti-myc antibody. (B) Changes in $[Ca^{2+}]_i$ in HEK-293 cells. HEK-293 cells were cotransfected with pcDNA3.1-myc-PMCA4b and pcDNA3.1-nNOS for 48 h, loaded with the Ca^{2+}-sensitive cell-permeable Fura-2-AM probe and then treated with thapsigargin and ionomycin. The changes in fluorescence intensity at 340/380 nm were recorded under a Nikon TE2000 fluorescence microscope. (C) Changes in of [NO]i in HEK-293 cells. HEK-293 cells were transfected with pcDNA3.1-myc-PMCA4b and pcDNA3.1-nNOS for 48 h, loaded with the NO-sensitive cell-permeable DAF-2-DA probe and then treated with thapsigargin and ionomycin. The changes in fluorescence intensity from 510–530 nm were recorded under a Nikon TE2000 fluorescence microscope. (D) Quantitative determination of PMCA and nNOS activity.

interaction between PMCA4b and nNOS.

The influence of lipid rafts on the interaction between PMCA4b and nNOS was also investigated. We found that pretreatment of the cells with MβCD abolished the interaction between PMCA4b and nNOS, which indicated that the integrity of the lipid raft microdomains is needed for the interaction of these two proteins.

DISCUSSION

Ca^{2+} is essential for regulating a large number of fundamental cellular physiologic functions (Carafoli, 2003); thus, the changes in $[Ca^{2+}]_i$ must be tightly regulated. Membrane proteins such as calcium ATPases (also known as calcium pumps) and sodium/calcium exchangers are responsible for transporting Ca^{2+} across the membrane (Brini and Carafoli, 2009). Calcium ATPases anchored to the plasma membrane (PMCA) have a high affinity for Ca^{2+} and they precisely control Ca^{2+} signals to ensure the accurate transmission (target/effector and amplitude/frequency) of the signals (Brini, 2009; Oceandy et al., 2010). In mammals, PMCAs are encoded by a multigene family (*ATP2B1–ATP2B4*) to form four isoforms: PMCA1, PMCA2, PMCA3, and PMCA4. PMCA1 and PMCA4 are ubiquitous, whereas PMCA2 and PMCA3 are much more restricted to certain tissues. Two main variants, denoted as PMCAa and PMCAb, were observed from the alternate splicing of the mRNA transcripts at the C-terminus splice site of PMCA (Kruger et al., 2009). More than 30 different spliced forms of PMCA have been identified (Guerini, 1998; Strehler and Zacharias, 2001), which have been associated with the high complexity and temporal/spatial specificity of the Ca^{2+} signals.

PMCA4 is ubiquitously expressed in mammalian cells and is regarded as a key modulator of Ca^{2+}-related signaling in neuronal cells (Kim et al., 1998; Schuh et al., 2001), cardiomyocytes (Oceandy et al., 2007), and endothelial cells (Holton et al., 2010). The PMCA4b splice variant contains a PDZ-binding

© Higher Education Press and Springer-Verlag Berlin Heidelberg 2013

motif that allows it to interact with the PDZ domains of other proteins. Several of these interacting proteins have been identified in neuronal cells, including membrane-associated guanylate kinase (MAGUK) (Kim et al., 1998), calcium/calmodulin-dependent serine protein kinase (CASK) (Schuh et al., 2003), Ania-3 (Sgambato-Faure et al., 2006), and nNOS (Schuh et al., 2001). The interaction between PMCA4b and nNOS has been investigated systematically by Neyses et al., (Schuh et

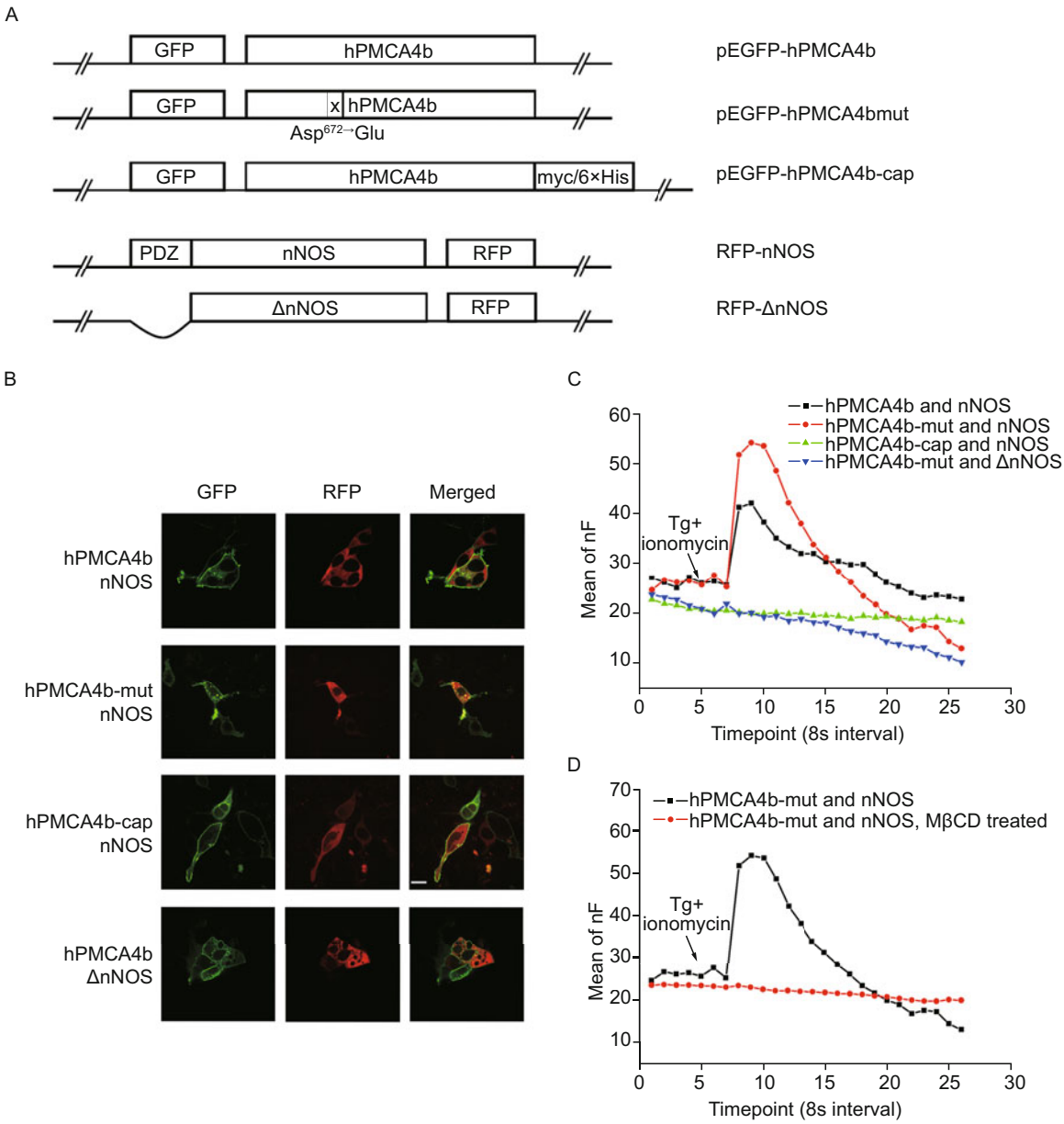

Figure 6. Changes in Ca^{2+}-induced fluorescence resonance energy transfer between PMCA4b and nNOS. (A) Plasmid constructs used in FRET. pEGFP-hPMCA4b containing full-length human PMCA4b sequences. pEGFP-hPMCA4b-mut carried an Asp^{672}→Glu mutation, which causes a ~90% decrease in ATPase activity. pEGFP-hPMCA4b-cap contains a myc/6× His tag that caps the PDZ-binding C-terminus of PMCA4b. pRFP-nNOS contains the full-length nNOS sequence. pRFP-ΔnNOS contains part of the nNOS sequence without an interacting PDZ domain (1–299 aa). (B) Expression and intracellular localization of fused proteins in HEK-293 cells. HEK-293 cells were transfected with the plasmids for 48 h, and then visualized under a PerkinElmer UltraVIEW VoX confocal microscope system. Bar, 15 μm. (C) Changes in FRET in HEK-293 cells. HEK-293 cells were transfected with the plasmids for 48 h, and then treated with thapsigargin and ionomycin. The changes in FRET between PMCA (green; donor) and nNOS (red; acceptor) were recorded under a Perkin Elmer UltraVIEW VoX confocal microscope system. Cells were imaged at 8 s-intervals for 208 s. The curves with different colors represent the changes in nF. (D) Disruption of lipid rafts blocked the occurrence of FRET. HEK-293 cells were transfected with pEGFP-hPMCA4b-mut and RFP-nNOS for 48 h, with and without MβCD pretreatment, and then treated with thapsigargin and ionomycin. The changes in FRET between PMCA and nNOS were recorded.

© Higher Education Press and Springer-Verlag Berlin Heidelberg 2013

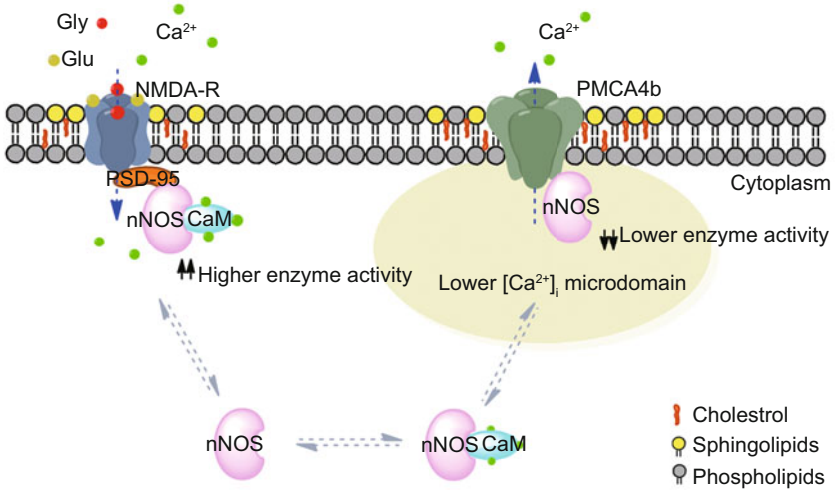

Figure 7. Activation and deactivation of nNOS in neurons. PMCA4b decreased the local $[Ca^{2+}]_i$ levels by transporting Ca^{2+} out of the cells , thereby downregulating the nNOS activity dynamically associated with PMCA4b via Ca^{2+}-dependent, PDZ domain–mediated protein–protein interactions. The lipid rafts rich in PMCA4b may act as platforms by which PMCA4b regulates nNOS activity.

al., 2001; Oceandy et al., 2007), and they hypothesized that PMCA4b may be the key modulator of nNOS deactivation (Mohamed et al., 2009, 2011). However, investigating the function of proteins and protein networks in the cell should be preferably performed *in vivo* to maintain the cellular context (Piehler, 2005).

Considering the highly dynamic nature of transmembrane proteins (Ciruela, 2008; Loura and Prieto, 2011; Miyawaki, 2011), we employed FRET instead of biochemical approaches to investigate the interaction between PMCA4b and nNOS in living cells. The results of the time-resolved FRET clearly indicated energy transfer between PMCA4b and nNOS, which suggests the occurrence of protein–protein interactions (Fig. 6). More importantly, we found that the interaction is highly dynamic. The transient FRET only occurs under high $[Ca^{2+}]_i$. No FRET was observed under basal $[Ca^{2+}]_i$ caused by PMCA activation. We also found that both the PDZ domain of nNOS and the PDZ-binding motif of PMCA4b are essential for the interaction in living cells, which is in accordance with the results obtained using cell-free systems (Schuh et al., 2001).

The interaction between PMCA4b and nNOS depends on $[Ca^{2+}]_i$; thus, we determined how Ca^{2+} modulates the protein–protein interactions. As a P-type ATPase, the C-terminus of PMCA has a self-inhibitory effect. Under physiologic conditions when certain cellular events increase the intracellular free Ca^{2+} concentrations , the Ca^{2+}-mediated binding of calmodulin to the C-terminus of PMCA prevents the self-inhibition, thereby activating PMCA (Falchetto et al., 1991; Falchetto et al., 1992; Kobe and Kemp, 1999). Using intramolecular FRET technology, Gerardo confirmed the rearrangement of the N- and the C-terminal segments of PMCA during activation (Corradi and Adamo, 2007). Based on these reports, we speculated that the Ca^{2+}-mediated rearrangement of PMCA provides the structural basis for the protein–protein interactions.

The present investigation found that the integrity of lipid rafts is necessary for the protein–protein interaction and the activation of PMCA4b and nNOS. The distribution of PMCA in the plasma membrane microdomains differs in different cell types. In endothelial cells, smooth muscle cells, and cardiac muscle cells, the PMCA4b is localized in the caveolae, a specialized subset of lipid rafts (Fujimoto, 1993; Hammes et al., 1998). Our results indicate that PMCA4b is relatively enriched in the lipid rafts of neuronal plasma membranes (Fig. 1C), which was in accordance with previous reports (Sepulveda et al., 2006). The partitioning of PMCA4b in lipid rafts suggests that it exerts certain functions related to lipid rafts. Lipid rafts are thought to dynamically organize cellular signaling events triggered by extracellular stimuli (Simons and Ikonen, 1997; Brown and London, 1998). A large number of signaling molecules are situated in these subcellular microdomains, and a considerable amount of molecular signal, including Ca^{2+}, may reach lipid rafts (Parton, 2001). In this regard, PMCA4b displays its key role, selecting the target for the calcium signal (Oceandy et al., 2010). A recent study revealed that lipid raftanchored PMCA has higher activity than PMCA localized in non-raft microdomains (Jiang et al., 2007). In addition to other cellular compartments, nNOS has also been shown to be localized to caveolae in several cell types including muscle cells (Stamler and Meissner, 2001; Cartwright et al., 2009). The caveolae of cardiomyocytes have been regarded as platforms for assembling PMCA4/nNOS/α1-syntrophin signaling complexes (Williams et al., 2006). Our findings further suggest the importance of lipid rafts for PMCA4/nNOS interaction in neuronal cells.

Controlling the local $[Ca^{2+}]_i$ has an important role during nNOS activation in neuronal cells. By interacting with scaffolding proteins such as PSD95, nNOS and NMDA-R form signaling complexes at the neuronal plasma membrane, where the Ca^{2+} influx rapidly activates nNOS (Brenman et al., 1996).

© Higher Education Press and Springer-Verlag Berlin Heidelberg 2013

Similar mechanisms may also be involved in the deactivation of nNOS. PMCA4b, which is enriched in lipid rafts with high Ca^{2+} affinity, changes into its active form under elevated $[Ca^{2+}]_i$ (Corradi and Adamo, 2007); thus, it interacts rapidly with nNOS via PDZ-related interactions. Activated PMCA4b rapidly decreases the local Ca^{2+}, which rapidly decreases nNOS activity. Lower local $[Ca^{2+}]_i$ also initiates the rearrangement of PMCA and releases the interaction with nNOS (Fig. 7).

In conclusion, we provide direct evidence that increasing $[Ca^{2+}]_i$ triggers a transient interaction between PMCA4b and nNOS in living cells, which depends on the integrity of lipid rafts. By transporting Ca^{2+} out of the cells, the PMCA4b enriched in lipid rafts decreases the local $[Ca^{2+}]_i$ levels, thereby downregulating the nNOS activity dynamically associated to PMCA4b via Ca^{2+}-dependent PDZ domain–mediated protein–protein interactions. Lipid rafts may act as platforms for the regulation of nNOS activity by PMCA4b, and the transient tethering of nNOS to PMCA4b is responsible for the rapid deactivation of nNOS.

MATERIALS AND METHODS

Antibodies and chemicals

Primary antibodies against PMCA1, PMCA2, PMCA3, and PMCA4 were obtained from Affinity Bioreagents. The primary antibodies against nNOS were from Cell Signaling Technology, whereas the primary antibodies against β-actin were from Santa Cruz. The primary antibodies against flotillin-1 were from BD Biosciences. HRP-, FITC-, and TRITC-conjugated secondary antibodies were from Santa Cruz. Dulbecco's modified Eagle's medium (DMEM), fetal bovine serum, cell culture supplements, TRIzol™, Lipofectamine™ 2000, and Fura-2-AM were from Invitrogen. DAF-2-DA, thapsigargin, and ionomycin were from Merck. All other chemicals were from Sigma.

Recombinant DNA constructs

The plasmids pCMV-hPMCA4b, pCMV-hPMCA4b-mut, and pCMV-hPMCA4b-cap were generously provided by Dr. Ludwig Neyses (University of Manchester, UK). The plasmids pcDNA3.1-nNOS and pEGFP-hPMCA4b were kindly provided by Dr. Rohini Kuner (University of Heidelberg, Germany) and Dr. Stanley A. Thayer (University of Minnesota, USA), respectively.

The pRFP-nNOS plasmid that expresses a fused RFP and rat nNOS protein was generated using the pDsRed/monomer C1 vector (Clontech) at the *Xho*I and *Eco*RI sites. The pRFP-ΔnNOS plasmid that expresses a fused RFP and rat nNOS protein without an interacting PDZ domain (1–299 aa) deleted was generated using the same method. The pEGFP-hPMCA4b plasmid that expresses a fused EGFP and human PMCA4b protein, the pEGFP-hPMCA4b-mut plasmid that expresses a fused EGFP and human PMCA4b protein with an Asp^{672}→Glu mutation, and the pEGFP-hPMCA4b-cap plasmid that expresses a fused protein EGFP and human PMCA4b protein with a myc/6× His tag at the PMCA4b C-terminus were generated using the pEGFP-N1 vector (Clontech) at the *Xho*I and *Bam*HI sites (Schuh et al., 2001). The pcDNA3.1-myc-hPMCA4b plasmid that expresses a myc-tagged human PMCA4b was constructed using a pcDNA3.1(-) vector at the *Bam*HI and *Kpn*I sites.

Cell culture and transfection

Primary cultures of cerebellar granule cells were prepared from 7-day-old Sprague–Dawley rat pups (Beijing Vital River Experimental Animal Center). The cerebella were dissected and trypsinized at 37°C for 20 min. Trypsinization was terminated using fetal bovine serum, and the cells were mechanically dissociated by pipetting up and down for 5 times. The cells were resuspended in high-glucose DMEM supplemented with 10% fetal bovine serum, penicillin (100 U/mL), streptomycin (100 μg/mL), and 25 mmol/L KCl, and were seeded into 35 mm-dishes previously coated with poly-d-lysine (100 μg/mL). The cells were maintained in a humidified incubator containing 5% CO_2 and 8% O_2 at 37°C. At 24 h after seeding, cytosine arabinoside (10 μmol/L) was added into the medium to inhibit the growth of non-neuronal cells. The cells were ready for use on the seventh day.

HEK-293 cells were grown in high-glucose DMEM supplemented with 10% fetal bovine serum, penicillin (100 U/mL), and streptomycin (100 μg/mL), and maintained in a humidified 5% CO_2/air incubator at 37°C. The cells were transfected with various vectors using Lipofectamine™ 2000 reagent. The cells were used for experiments at 48 h after transfection.

Isolation of synaptic plasma membrane and separation of lipid rafts

The protocol for synaptic plasma membrane (SPM) isolation was kindly provided by Dr. Pingsheng Liu (Institute of Biophysics, CAS). Briefly, the brains of six Sprague–Dawley rats were collected and kept in 0.3 mol/L sucrose on ice. The forebrains were homogenized using 20 strokes in a 50 mL-glass dounce, and the homogenate was centrifuged at 800 g for 20 min. The supernatant was collected and centrifuged at 9000 g for 20 min. The pellet was washed once with 0.3 mol/L sucrose, incubated in 0.03 mol/L sucrose for 20 min on ice, and then centrifuged at 14,000 g for 20 min. The pellet was resuspended in double distilled water, homogenized using 10 strokes in a glass dounce, and was adjusted to 1.1 mol/L sucrose and 5 mmol/L Tris (pH 7.5) in a final volume of 15 mL. The sample was overlaid with 14 mL of 0.8 mol/L sucrose and 5 mL of 0.3 mol/L sucrose, and centrifuged at 84,000 g for 2 h in SW40 rotor (Beckman). Crude SPM was collected from the interface of 0.8 mol/L to 1.1 mol/L sucrose, diluted with ice-cold water (1:3), and centrifuged at 200,000 g in an SW40 rotor for 40 min. The resulting SPM was used to isolate lipid rafts following the method described by Sepúlveda et al. (2006). Thirteen fractions obtained from density gradient centrifugation were collected and kept at -80°C for subsequent western blot analysis.

RT-PCR

The cerebral cortex, cerebellar cortex, hippocampus, and corpus striatum were dissected from Sprague–Dawley rats, and the total RNA from each tissue was isolated using TRIzol reagent. cDNA was synthesized using a random primer and an Omniscript reverse transcription kit (Qiagen). PMCA1, PMCA2, PMCA3, and PMCA4 cDNA were amplified using the following primers (Mamic et al., 2000; Tachibana et al., 2004): PMCA1 sense 5′-GGCGACTTTGGCATCACACT-3′ and anti-sense 5′-TTTCAACTTGGTGCAAATTCCA-3′; PMCA2 sense 5′-ATCCAGACACAGATCCGCGTCGTG-3′ and anti-sense 5′-GATTTGCTCGTGTCGGTCGTCAGG-3′; PMCA3 sense 5′-ACCAGTGTATGTGCAGTACTTTGTG-3′ and anti-sense 5′-CTAG-

© Higher Education Press and Springer-Verlag Berlin Heidelberg 2013

GTAGGACTGAACCACTGTCAT-3′; PMCA4 sense 5′-GTCTATCCTCACAGTCCTCATCCT-3′ and anti-sense 5′-CTTTACAGAGTAGGCCAACGAGAT-3′. β-Actin was amplified as the housekeeping control using the primers sense 5′-GATGACCCAGATCATGTTTGA-3′ and anti-sense 5′-GGGCACAGTGTGGGTGAC-3′. The RT-PCR products were electrophoresed on 2% agarose gel and visualized after ethidium bromide staining.

Western blot analysis

The cerebral cortex, cerebellar cortex, hippocampus, and corpus striatum were obtained from adult Sprague Dawley rats. Soluble proteins from the tissues and cells were extracted with ice-cold RIPA buffer (50 mmol/L Tris/HCl, pH 7.4, 150 mmol/L NaCl, 1% NP-40, 0.25% sodium deoxycholate, 1 mmol/L EDTA, 1 mmol/L NaF, and proteinase inhibitor cocktails). The protein concentrations were measured using a BCA protein assay kit (Pierce). Approximately 20 μg of each sample was subjected to SDS-PAGE and electroblotted onto PVDF membranes (GE). After blocking with 5% nonfat dry milk in TBST (10 mmol/L Tris/HCl, pH 7.4, 150 mmol/L NaCl, 0.1% Tween-20) at room temperature for 1 h, the membranes were incubated with proper primary antibodies overnight at 4°C. After washing with TBST, the membranes were incubated with HRP-conjugated secondary antibodies for 1 h at room temperature. The immunoblots were visualized using a Super-Signal West Pico chemiluminescent substrate system (Pierce).

Immunofluorescence microscopy

The cells were fixed in 4% paraformaldehyde for 30 min at room temperature and were permeabilized with 1% Triton X-100 for 10 min. After blocking with 5% goat serum, the cells were incubated overnight at 4°C with primary antibodies in PBS. The cells were incubated for 1 h with FITC- and TRITC-conjugated secondary antibodies at 37°C before they were observed under an Olympus FV500 laser confocal scanning microscope. In some experiments, the cells were pretreated with 10 mmol/L methyl-β-cyclodextrin (MβCD) for 30 min to disrupt the lipid rafts (Zhang et al., 2009).

Förster resonance energy transfer (FRET)

FRET was employed to determine the changes in the protein–protein interaction between PMCA4b and nNOS. HEK-293 cells were transfected or cotransfected with the pEGFP-hPMCA4b, pRFP-nNOS, pEGFP-hPMCA4b-mut, pEGFP-hPMCA4b-cap, or the pRFP-ΔnNOS plasmids. They were then seeded onto 30 mm-glass coverslips at 3 × 10_4 cell/well, and maintained at 37°C for 48 h. Subsequently, the cells were incubated in isosmotic buffer containing 145 mmol/L N-methyl-d-glucamine, 5 mmol/L KCl, 1 mmol/L $MgCl_2$, 1 mmol/L $CaCl_2$, 10 mmol/L d-glucose, 100 μmol/L l-arginine, and 10 mmol/L HEPES, pH 7.4. The cells were treated with 1 μmol/L thapsigargin and 50 nmol/L ionomycin to induce a transient increase in $[Ca^{2+}]_i$. In some experiments, the cells were pretreated with 10 mmol/L MβCD for 30 min to impair the lipid raft microdomains before the thapsigargin/ionomycin treatment.

The changes in FRET were recorded using an UltraVIEW VoX laser confocal scanning microscope system (Perkin Elmer) equipped with a 60×, 1.4 NA oil immersion objective lens and a cultivation chamber fitted with a temperature-control and CO_2-control device (Tokai Hit, 37°C, 5% CO_2). The cells were imaged at 8 s-intervals for 208 s. EGFP-tagged proteins were excited at 488 nm and their emissions were detected at 530 nm. RFP-tagged proteins were excited at 561 nm and their emissions were detected at 615 nm. Cells transfected with empty vector (pcDNA3.1) were used for background correction. The FRET method was carried out as described by Youvan (1997), with minor modifications. Cells expressing donor and acceptor construct were used to compensate for the signal in the FRET channel (excitation: 488 nm, emission: 615 nm) for spectral bleed through and cross-excitation (a and b value).

net FRET (nF) was calculated using the following equation:

net FRET = FRET signal – (a × RFP signal) – (b × EGFP signal).

Both RFP and EGFP signals were observed in the cell, and appropriate percentages of these two signals must be subtracted from any signal measured in the FRET channel. This procedure was done on the entire image using some type of image arithmetic, or it can be done on a pixel-by-pixel basis at specific cellular substructures. The images and data analysis were processed with Volocity software (Perkin Elmer).

$[Ca^{2+}]_i$ and $[NO]_i$ assays

The $[Ca^{2+}]_i$ of individual cells and PMCA activity were assayed using Fura-2-AM, as previously described (Zhang et al., 2009). NO production in individual cells was monitored using the NO-sensitive fluorescence probe DAF-2-DA (Kojima et al., 1998; Zhou and He, 2011). The primary cerebellar granule cells or HEK-293 cells were loaded with 2 μmol/L Fura-2-AM or 1 μmol/L DAF-2-DA in serum-free DMEM for 30 min at 37°C, and then incubated in isosmotic buffer containing 145 mmol/L N-methyl-d-glucamine, 5 mmol/L KCl, 1 mmol/L $MgCl_2$, 1 mmol/L $CaCl_2$, 10 mmol/L d-glucose, 100 μmol/L l-arginine, and 10 mmol/L HEPES, pH 7.4. We added 100 μmol/L glutamate, 10 μmol/L of glycine plus 1 μmol/L of thapsigargin to the cerebellar granule cells to induce a glutamate receptor–coupled increase in $[Ca^{2+}]_i$, whereas 1 μmol/L thapsigargin and 50 nmol/L ionomycin were added to the HEK-293 cells to induce a transient increase in $[Ca^{2+}]_i$ (Zhang et al., 2009). The changes in fluorescence intensity of Fura-2-loaded cells at 340 nm/380 nm excitation and 510 nm emission wavelengths and those of DAF-2-loaded cells at 490 nm excitation and 515 nm emission wavelengths were recorded under a Nikon TE2000 inverted epifluorescence microscope equipped with a 40× oil immersion objective lens and a Sutter filter wheel. In all experiments, the objective was focused on cell somata rather than neurites. The time courses for $[Ca^{2+}]_i$ and $[NO]_i$ were plotted from a minimum of 20 randomly selected cell somata.

ACKNOWLEDGEMENTS

This work was supported by grants from the National Basic Research Program of China (Grant Nos. 2010CB833701 and 2012CB934003) and the National Natural Science Foundation of China (Grant No. 31070736). We would like to thank Profs. Pingsheng Liu, Youguo Huang, and Xujia Zhang (Institute of Biophysics, CAS) for their valuable suggestions and discussions. We are also indebted to Wenmin Zhong (Institute of Biophysics, CAS) for her technical assistance.

REFERENCES

Adamo, H.P., Filoteo, A.G., Enyedi, A., and Penniston, J.T. (1995). Mu-

© Higher Education Press and Springer-Verlag Berlin Heidelberg 2013

tants in the putative nucleotide-binding region of the plasma membrane Ca(2+)-pump. A reduction in activity due to slow dephosphorylation. J Biol Chem 270, 30111–30114.

Alderton, W.K., Cooper, C.E., and Knowles, R.G. (2001). Nitric oxide synthases: structure, function and inhibition. Biochem J 357, 593–615.

Brenman, J.E., Chao, D.S., Gee, S.H., McGee, A.W., Craven, S.E., Santillano, D.R., Wu, Z., Huang, F., Xia, H., Peters, M.F., et al. (1996). Interaction of nitric oxide synthase with the postsynaptic density protein PSD-95 and alpha1-syntrophin mediated by PDZ domains. Cell 84, 757–767.

Brini, M. (2009). Plasma membrane Ca(2+)-ATPase: from a housekeeping function to a versatile signaling role. Pflugers Arch 457, 657–664.

Brini, M., and Carafoli, E. (2009). Calcium pumps in health and disease. Physiol Rev 89, 1341–1378.

Brown, D.A., and London, E. (1998). Functions of lipid rafts in biological membranes. Annu Rev Cell Dev Biol 14, 111–136.

Calabrese, V., Mancuso, C., Calvani, M., Rizzarelli, E., Butterfield, D.A., and Stella, A.M. (2007). Nitric oxide in the central nervous system: neuroprotection versus neurotoxicity. Nat Rev Neurosci 8, 766–775.

Carafoli, E. (2003). The calcium-signalling saga: tap water and protein crystals. Nat Rev Mol Cell Biol 4, 326–332.

Cartwright, E.J., Oceandy, D., and Neyses, L. (2009). Physiological implications of the interaction between the plasma membrane calcium pump and nNOS. Pflugers Arch 457, 665–671.

Ciruela, F. (2008). Fluorescence-based methods in the study of protein-protein interactions in living cells. Curr Opin Biotechnol 19, 338–343.

Corradi, G.R., and Adamo, H.P. (2007). Intramolecular fluorescence resonance energy transfer between fused autofluorescent proteins reveals rearrangements of the N- and C-terminal segments of the plasma membrane Ca2+ pump involved in the activation. J Biol Chem 282, 35440–35448.

Dudek, H., Datta, S.R., Franke, T.F., Birnbaum, M.J., Yao, R., Cooper, G.M., Segal, R.A., Kaplan, D.R., and Greenberg, M.E. (1997). Regulation of neuronal survival by the serine-threonine protein kinase Akt. Science 275, 661–665.

Falchetto, R., Vorherr, T., Brunner, J., and Carafoli, E. (1991). The plasma membrane Ca2+ pump contains a site that interacts with its calmodulin-binding domain. J Biol Chem 266, 2930–2936.

Falchetto, R., Vorherr, T., and Carafoli, E. (1992). The calmodulin-binding site of the plasma membrane Ca2+ pump interacts with the transduction domain of the enzyme. Protein Sci 1, 1613–1621.

Fujimoto, T. (1993). Calcium pump of the plasma membrane is localized in caveolae. J Cell Biol 120, 1147–1157.

Guerini, D. (1998). The significance of the isoforms of plasma membrane calcium ATPase. Cell Tissue Res 292, 191–197.

Guix, F.X., Uribesalgo, I., Coma, M., and Munoz, F.J. (2005). The physiology and pathophysiology of nitric oxide in the brain. Prog Neurobiol 76, 126–152.

Hammes, A., Oberdorf-Maass, S., Rother, T., Nething, K., Gollnick, F., Linz, K.W., Meyer, R., Hu, K., Han, H., Gaudron, P., et al. (1998). Overexpression of the sarcolemmal calcium pump in the myocardium of transgenic rats. Circ Res 83, 877–888.

Holton, M., Mohamed, T.M., Oceandy, D., Wang, W., Lamas, S., Emerson, M., Neyses, L., and Armesilla, A.L. (2010). Endothelial nitric oxide synthase activity is inhibited by the plasma membrane calcium ATPase in human endothelial cells. Cardiovasc Res 87, 440–448.

Jiang, L., Fernandes, D., Mehta, N., Bean, J.L., Michaelis, M.L., and Zaidi, A. (2007). Partitioning of the plasma membrane Ca2+-ATPase into lipid rafts in primary neurons: effects of cholesterol depletion. J Neurochem 102, 378–388.

Kim, E., DeMarco, S.J., Marfatia, S.M., Chishti, A.H., Sheng, M., and Strehler, E.E. (1998). Plasma membrane Ca2+ ATPase isoform 4b binds to membrane-associated guanylate kinase (MAGUK) proteins via their PDZ (PSD-95/Dlg/ZO-1) domains. J Biol Chem 273, 1591–1595.

Kim, W.K., Choi, Y.B., Rayudu, P.V., Das, P., Asaad, W., Arnelle, D.R., Stamler, J.S., and Lipton, S.A. (1999). Attenuation of NMDA receptor activity and neurotoxicity by nitroxyl anion, NO. Neuron 24, 461–469.

Kobe, B., and Kemp, B.E. (1999). Active site-directed protein regulation. Nature 402, 373–376.

Kojima, H., Nakatsubo, N., Kikuchi, K., Urano, Y., Higuchi, T., Tanaka, J., Kudo, Y., and Nagano, T. (1998). Direct evidence of NO production in rat hippocampus and cortex using a new fluorescent indicator: DAF-2 DA. Neuroreport 9, 3345–3348.

Kruger, W.A., Yun, C.C., Monteith, G.R., and Poronnik, P. (2009). Muscarinic-induced recruitment of plasma membrane Ca2+-ATPase involves PSD-95/Dlg/Zo-1-mediated interactions. J Biol Chem 284, 1820–1830.

Loura, L.M., and Prieto, M. FRET in Membrane Biophysics: An Overview. (2011). Front Physiol 2, 82.

Mamic, T.M., Holman, N.A., Roberts-Thomson, S.J., and Monteith, G.R. (2000). PMCA1 mRNA expression in rat aortic myocytes: a real-time RT-PCR study. Biochem Biophys Res Commun 276, 1024–1027.

Miyawaki, A. Development of probes for cellular functions using fluorescent proteins and fluorescence resonance energy transfer. (2011) Annu Rev Biochem 80, 357–373.

Mohamed, T.M., Oceandy, D., Prehar, S., Alatwi, N., Hegab, Z., Baudoin, F.M., Pickard, A., Zaki, A.O., Nadif, R., Cartwright, E.J., et al. (2009). Specific role of neuronal nitric-oxide synthase when tethered to the plasma membrane calcium pump in regulating the beta-adrenergic signal in the myocardium. J Biol Chem 284, 12091–12098.

Mohamed, T.M., Oceandy, D., Zi, M., Prehar, S., Alatwi, N., Wang, Y., Shaheen, M.A., Abou-Leisa, R., Schelcher, C., Hegab, Z., et al. (2011). Plasma membrane calcium pump (PMCA4)-neuronal nitric-oxide synthase complex regulates cardiac contractility through modulation of a compartmentalized cyclic nucleotide microdomain. J Biol Chem 286, 41520–41529.

Moncada, S., and Bolanos, J.P. (2006). Nitric oxide, cell bioenergetics and neurodegeneration. J Neurochem 97, 1676–1689.

Moro, M.A., Cardenas, A., Hurtado, O., Leza, J.C., and Lizasoain, I. (2004). Role of nitric oxide after brain ischaemia. Cell Calcium 36, 265–275.

Oceandy, D., Mohamed, T.M., Cartwright, E.J., and Neyses, L. (2010). Local signals with global impacts and clinical implications: lessons from the plasma membrane calcium pump (PMCA4). Biochim Biophys Acta 1813, 974–978.

Oceandy, D., Stanley, P.J., Cartwright, E.J., and Neyses, L. (2007). The

© Higher Education Press and Springer-Verlag Berlin Heidelberg 2013

regulatory function of plasma-membrane Ca(2+)-ATPase (PMCA) in the heart. Biochem Soc Trans 35, 927–930.

Pacher, P., Beckman, J.S., and Liaudet, L. (2007). Nitric oxide and peroxynitrite in health and disease. Physiol Rev 87, 315–424.

Parton, R.G. (2001). Cell biology. Life without caveolae. Science 293, 2404–2405.

Piehler, J. (2005). New methodologies for measuring protein interactions in vivo and in vitro. Curr Opin Struct Biol 15, 4–14.

Sagami, I., Daff, S., and Shimizu, T. (2001). Intra-subunit and inter-subunit electron transfer in neuronal nitric-oxide synthase: effect of calmodulin on heterodimer catalysis. J Biol Chem 276, 30036–30042.

Schuh, K., Uldrijan, S., Gambaryan, S., Roethlein, N., and Neyses, L. (2003). Interaction of the plasma membrane Ca2+ pump 4b/CI with the Ca2+/calmodulin-dependent membrane-associated kinase CASK. J Biol Chem 278, 9778–9783.

Schuh, K., Uldrijan, S., Telkamp, M., Rothlein, N., and Neyses, L. (2001). The plasmamembrane calmodulin-dependent calcium pump: a major regulator of nitric oxide synthase I. J Cell Biol 155, 201–205.

Sepulveda, M.R., Berrocal-Carrillo, M., Gasset, M., and Mata, A.M. (2006). The plasma membrane Ca2+-ATPase isoform 4 is localized in lipid rafts of cerebellum synaptic plasma membranes. J Biol Chem 281, 447–453.

Sgambato-Faure, V., Xiong, Y., Berke, J.D., Hyman, S.E., and Strehler, E.E. (2006). The Homer-1 protein Ania-3 interacts with the plasma membrane calcium pump. Biochem Biophys Res Commun 343, 630–637.

Simons, K., and Ikonen, E. (1997). Functional rafts in cell membranes. Nature 387, 569-572.

Stamler, J.S., and Meissner, G. (2001). Physiology of nitric oxide in skeletal muscle. Physiol Rev 81, 209–237.

Strehler, E.E., and Zacharias, D.A. (2001). Role of alternative splicing in generating isoform diversity among plasma membrane calcium pumps. Physiol Rev 81, 21–50.

Tachibana, T., Ogura, H., Tokunaga, A., Dai, Y., Yamanaka, H., Seino, D., and Noguchi, K. (2004). Plasma membrane calcium ATPase expression in the rat spinal cord. Brain Res Mol Brain Res 131, 26–32.

Torreilles, F., Salman-Tabcheh, S., Guerin, M., and Torreilles, J. (1999). Neurodegenerative disorders: the role of peroxynitrite. Brain Res Brain Res Rev 30, 153–163.

Tran, M.H., Yamada, K., Nakajima, A., Mizuno, M., He, J., Kamei, H., and Nabeshima, T. (2003). Tyrosine nitration of a synaptic protein synaptophysin contributes to amyloid beta-peptide-induced cholinergic dysfunction. Mol Psychiatry 8, 407–412.

Williams, J.C., Armesilla, A.L., Mohamed, T.M., Hagarty, C.L., McIntyre, F.H., Schomburg, S., Zaki, A.O., Oceandy, D., Cartwright, E.J., Buch, M.H., et al. (2006). The sarcolemmal calcium pump, alpha-1 syntrophin, and neuronal nitric-oxide synthase are parts of a macromolecular protein complex. J Biol Chem 281, 23341–23348.

Youvan, D.C., Silva, C.M., Bylina, E.J., Coleman, W.J., Dilworth, M.R., and Yang, M.M. (1997). Calibration of fluorescence resonance energy transfer in microscopy using genetically engineered GFP derivatives on Nickel chelating beads. Biotechnology et alia 3, 1–18.

Zhang, J., Xiao, P., and Zhang, X. (2009). Phosphatidylserine externalization in caveolae inhibits Ca2+ efflux through plasma membrane Ca2+-ATPase in ECV304. Cell Calcium 45, 177–184.

Zhou, L., and Zhu, D.Y. (2009). Neuronal nitric oxide synthase: structure, subcellular localization, regulation, and clinical implications. Nitric Oxide 20, 223–230.

Zhou, X., and He, P. (2011). Improved measurements of intracellular nitric oxide in intact microvessels using 4,5-diaminofluorescein diacetate. Am J Physiol Heart Circ Physiol 301, H108–114.

© Higher Education Press and Springer-Verlag Berlin Heidelberg 2013